J. Biochem. 132, 433–439 (2002)

Spectroscopic Analysis of Recombinant Rat Histidine Decarboxylase[1]

María Teresa Olmo,* Francisca Sánchez-Jiménez,*,[2] Miguel Angel Medina,* and Hideyuki Hayashi†

**Department of Molecular Biology and Biochemistry, Faculty of Sciences, University of Málaga, 29071 Málaga, Spain; and †Department of Biochemistry, Osaka Medical College, Takatsuki, Osaka 569-8686*

Received April 26, 2002; accepted July 2, 2002

Mammalian histidine decarboxylases have not been characterized well owing to their low amounts in tissues and instability. We describe here the first spectroscopic characterization of a mammalian histidine decarboxylase, *i.e.* a recombinant version of the rat enzyme purified from transformed *Escherichia coli* cultures, with similar kinetic constants to those reported for mammalian histidine decarboxylases purified from native sources. We analyzed the absorption, fluorescence and circular dichroism spectra of the enzyme and its complexes with the substrate and substrate analogues. The pyridoxal-5′-phosphate-enzyme internal Schiff base is mainly in an enolimine tautomeric form, suggesting an apolar environment around the coenzyme. Michaelis complex formation leads to a polarized, ketoenamine form of the Schiff base. After transaldimination, the coenzyme–substrate Schiff base exists mainly as an unprotonated aldimine, like that observed for dopa decarboxylase. However, the coenzyme–substrate Schiff base suffers greater torsion than that observed in other L-amino acid decarboxylases, which may explain the relatively low catalytic efficiency of this enzyme. The active center is more resistant to the formation of substituted aldamines than the prokaryotic homologous enzyme and other L-amino acid decarboxylases. Characterization of the similarities and differences of mammalian histidine decarboxylase with respect to other homol-ogous enzymes would open new perspectives for the development of new and more specific inhibitors with pharmacological potential.

Key words: catalytic mechanism, histamine, histidine decarboxylase, pyridoxal-5′-phosphate-dependent enzyme.

Mammalian L-amino acid decarboxylases (L-aaDCs) are mainly PLP-dependent enzymes. Based on their primary sequence, Sandmeier et al. (*1*) deduced four different evolutionary groups for L-aaDCs; among them, histidine decarboxylase (HDC), dopa decarboxylase (DDC), and glutamate decarboxylase (GDC) belong to group II, bacterial ornithine decarboxylase (ODC) to group III, and mammalian ODC to group IV. The four different fold types predicted for the PLP-dependent family of enzymes have been reviewed by Jansonius (*2*). HDC, DDC, GDC, and bacterial ODC belong to fold-type I (aspartate aminotransferase being the prototype), whereas mammalian ODC belongs to fold-type III. The structures of bacterial (*3*) and mammalian (*4, 5*) ODCs and DDC (*6*) have recently been solved.

In spite of the structural differences between group II/III and group IV L-aaDCs, current knowledge indicates that a similar catalytic mechanism has evolved from two different fold types (*4*). In decarboxylases, once the Michaelis complex is formed, transaldimination leads to the external aldimine with orientation of the α-carboxylate perpendicular to the pyridine ring, followed by the release of CO_2 and the formation of a quinonoid intermediate (*7*). However, some differences among the different enzymes, such as stereochemistry (*4*) and the protonation state of the intermediates, can be revealed when they are analyzed more deeply from a mechanistic point of view (*4, 8–18*).

PLP-dependent histidine decarboxylase activities have been detected in Gram negative bacteria (*19*) and mammals (*20*). However, the structure/function relationship and the catalytic mechanism of mammalian HDC have been poorly characterized; this is mainly due to the fact that the mammalian enzymes are very scarce and unstable proteins, and at least in mouse, the enzyme has been shown to be post-translationally processed to render it active (*20–27*). In rat and mouse, the N- and C-termini of the mature sub-

[1]This work was supported by Grants SAF2001-1889 (Plan Nacional I+D, Spain) and CIV-267 (PAI, Andalusia). This work was also supported in part by a Grant-in-Aid for Scientific Research on Priority Areas (No. 13125101) and one for Scientific Research (No. 13680697) to H.H. from the Japan Society for the Promotion of Science. MTO was a fellowship recipient from the Ramón Areces Foundation.

[2]To whom correspondence should be addressed. Tel: +34-952-131674, Fax: +34-952-132000, E-mail: kika@uma.es

[3]Actually, the difference is more than 30-fold taking into account the temperatures used for the measurements (25°C for the stopped-flow experiment and 37°C for assaying of the enzymatic activity).

Abbreviations: PLP, pyridoxal 5′-phosphate; HDC, histidine decarboxylase [EC 4.1.1.22]; DOPA, L-3,4-dihydroxyphenylalanine; DDC, aromatic L-amino acid decarboxylase or DOPA decarboxylase [EC 4.1.1.28]; GDC, glutamate decarboxylase [EC 4.1.1.15]; ODC, ornithine decarboxylase [EC 4.1.1.17]; L-aaDCs, L-amino acid decarboxylases; HisOMe, L-histidine methyl ester, DTT, dithiothreitol; k_{cat}, turnover number; PEG-300, polyethylenglycol-300; UV/Vis, ultraviolet/visible.

unit remain unknown, and active enzymes with subunit molecular weights of 53 kDa to 64 kDa have been observed in different cell types (*20–27*).

The product of HDC catalysis, histamine, is a biogenic amine related to important physiological and pathological processes: neurotransmission, gastric secretion, anaphylactic reactions, and cell growth. At present, therapies against undesirable effects of histamine mainly involve the blockage of histamine receptors by antagonists. Characterization of the mammalian HDC structure and catalytic mechanism, and the differences with respect to homologous enzymes, could open new perspectives for the development of new and more selective inhibitors acting specifically on the histamine synthesis in different organisms. Similar strategies have been adopted for other L-amino acid decarboxylases; their structural and mechanistic characterization has encouraged the development of specific and effective drugs (*5, 6*).

In the present study, we used an active recombinant version of rat HDC purified from transformed *Escherichia coli* cultures in the milligram scale. This allowed us to perform physicochemical characterization of this mammalian enzyme. We observed the enzymatic activity, and obtained absorption, fluorescence and CD spectra of the recombinant purified protein and its complexes with the substrate and substrate analogues, and compared the properties of the enzyme with those of other homologous decarboxylases.

EXPERIMENTAL PROCEDURES

Preparation of a Recombinant Enzyme Cell-Free Extract—The active versions of rat HDC were generated as follows. An insert containing the rat HDC ORF fragment (amino acids 1 to 512) flanked by *Bam*HI restriction sites was generated by PCR using oligonucleotide 5′-CGCGGGATTGGATCCCATATGATGGAGCC-3′ as a sense primer, and oligonucleotide H2 and the 1/512 HDC recombinant plasmid, which were both reported previously (*21*), as the other primer and the template, respectively. The PCR product was *Bam*HI-digested and ligated to *Bam*HI-digested pGEX6P-1. The insert was obtained from this plasmid and subcloned again into *Bam*HI-digested pET-11a (Novagen, Madison, WI). Recombinant plasmids pGEX6P-1/HDC1/512 and pET-11a/HDC1/512 were used to transform the BL21 and BL21(DE3)pLysS *E. coli* strains, respectively. In the former case, 200 ml of culture was used for each purification experiment. BL21 cells containing the recombinant plasmid were grown at 37°C until the OD_{600} reached 1.3–1.5. Induction was carried out for 22–23 h at 10°C with 5 μM IPTG. 1/512 HDC was released from the fusion protein bound to the affinity chromatography support by digestion with the Pre-Scission™ protease supplied with the kit. In the case of the recombinant pET plasmid, the purification procedure started from 10 liters of a transformed cell culture. The culture was grown at 37°C until the OD_{600} reached 0.6. Production of HDC was induced at this stage by the addition of 1 mM IPTG. The culture was switched to 30°C and the bacterial growth was continue for 3 h. Cells were harvested by centrifugation and stored at –20°C. Bacterial pellets were resuspended in 160–180 ml of 20 mM potassium phosphate (pH 7.0) containing 2 mM EDTA, 5 μM PLP, and 1% PEG-300, and then sonicated.

Enzyme Purification Procedures—The procedure for purification of the recombinant HDC was based on the procedures for native HDC from fetal rat liver (*20*) and recombinant DDC from transformed *E. coli*. (*9*). The purification procedure started with the pET-11a/HDC1/512 transformed BL21(DE3)pLysS cell-free extract. Solid ammonium sulfate was added to 25% saturation. After centrifugation to remove the precipitates, the supernatant was loaded onto a Phenyl-Sepharose CL-4B column (2.5 × 25 cm; Pharmacia Biotech, Sweden). The column was washed with a linear gradient from 20 mM potassium phosphate (pH 7.0, containing 25% saturating ammonium sulfate) to 1 mM potassium phosphate (pH 7.0). Both buffers contained 0.1 mM DTT and 5 μM PLP as stabilizers. HDC was eluted with the last buffer supplemented with 1% PEG-300. Fractions containing HDC were concentrated with Amicon ultrafiltration cells, and then loaded onto a DEAE-Toyopearl 650M (Tosoh, Tokyo) column equilibrated with 5 mM potassium phosphate (pH 7.0), 0.1 mM DTT, 5 μM PLP, 1% PEG-300 (buffer P). A linear gradient of NaCl, 0 to 0.2 M, was applied. HDC was eluted approximately at 0.1 M NaCl. HDC-containing fractions were further purified by hydroxyapatite chromatography (HTP, BioRad). Adsorption took place in buffer P, and elution was performed by increasing the buffer potassium phosphate concentration from 5 to 200 mM. HDC protein in fractions was detected by SDS/PAGE and Western blotting, using antibodies raised against a glutathione-S-transferase–1/512-HDC recombinant version (Spanish Patent 980019). The HDC protein concentration was estimated at 280 nm assuming the molar extinction coefficient calculation described previously for PLP-dependent enzymes (*28*). HDC activity was measured as the release of $^{14}CO_2$ from [1-^{14}C]-labeled histidine at 37°C, as reported previously (*19*). To avoid interference by free PLP with the spectroscopic analysis, the final purified preparations were always submitted to exclusion gel chromatography (Sephadex-G25 medium) in 50 mM Pipes buffer (different pH values, as indicated in the following sections) just before spectroscopic measurements.

Spectrophotometric Measurements—Absorption and fluorescence spectra were obtained with a Hitachi U-3300 spectrophotometer and 850 fluorescence spectrophotometer, respectively. CD spectroscopy was carried out on a Jasco J-600 spectropolarimeter, as reported previously (*8*). Analogues were used at a final concentration of 1 mM. The enzyme concentration used for these experiments was 9 μM. Stopped-flow spectrophotometry was performed with an Applied Photophysics stopped-flow SF.17MW spectrophotometer at 25°C. The dead time for this system was 2.3 ms under the pressure of 600 kPa. L-histidine and L-histidine methyl ester (HisOMe) were purchased from Nacalai Chemicals (Kyoto).

RESULTS AND DISCUSSION

General Observations on Purified Preparations—After the four-step purification procedure described under Experimental Procedures for the version encoded by the pET-11a/HDC1/512 recombinant plasmid, a 59 kDa band was observed as the major signal (more than 95%) on Coomassie Blue staining of the SDS-PAGE gels and image analysis (Fig. 1). This size corresponds to the predicted monomer molecular weight. This band was recognized by polyclonal antibodies raised against a fusion protein containing resi-

dues 1–512 of the HDC sequence. The maximum yield obtained with this procedure was 4 mg of HDC from 10 liters of bacterial culture (30 g wet weight of cells). This result is similar to that obtained for recombinant GDC expressed in a similar way using a pET-plasmid system (*14*). A high degree of purification was also obtained with the recombinant pGEX6P-1/HDC1/512 plasmid. However, there were difficulties in scaling up the protocol. Since some of the spectroscopic techniques used in this work require high quantities of highly purified protein, we had to carry out all spectroscopic measurements with the enzyme obtained by the former method.

The length of the recombinant polypeptide (from residue 1 to residue 512, 58 kDa) was chosen on the bases of previous reports indicating that recombinant 54 and 64 kDa versions of mouse HDC expressed in insect cells exhibit similar activities and intracellular localization (*29*). In addition, using recombinant versions of rat HDC expressed in transfected COST cells, Fleming and Wang (*26*) found that the truncated version showing the highest activity was obtained from a plasmid encoding residues 1–516, suggesting that it should be very similar to any of the different fully active polypeptides observed *in vivo* (*25, 27*). Both 1–516 and 1–512 have lost the same motifs, the PEST regions and the endoplasmic reticulum signaling domain present in the C-terminus (*22, 26*).

The estimated k_{cat} and K_m of the final 1/512 purified preparation were 0.077 s^{-1} and 0.4 mM, respectively, at 37°C; which are both in the order of the reported values for HDC purified from fetal rat liver and other mammalian tissues (*20, 24*). These results indicate that the recombinant 1/512 version (residues 1–512) must also be very similar to the mature 54 kDa version detected *in vivo*, and reinforce the previous idea that the mammalian enzyme is less efficient than both rat DDC (*20*) and HDC from Gram-negative bacteria (*19*), the estimated k_{cat} values being 1.67 and 204 s^{-1}, respectively.

Structure of the Internal Schiff Base—The absorption spectra of PLP-bound L-aaDCs have two maximum peaks around 335 and 425 nm, which are generally ascribed to enolimine (A) and ketoenamine (B) tautomers, respectively, of the Schiff base (aldimine) formed between PLP and a lysine residue of the protein (*8, 9, 14, 18*; for the structure, see Scheme 1). In the case of HDC, the absorption at 335 nm is twice as high as that at 425 nm at both pH 7 (Fig. 2, solid line) and pH 6 (not shown). A similar absorption spectrum was obtained with rat DDC (*8, 9*). The absorption band at around 330 nm also arises from the structures of 3-hydroxypyridine with no conjugated substituent at the 4-position, such as substituted aldamines. Fluorescence spectrometry has often been used to distinguish the two structures, *i.e.* the substituted aldamine and enolimine tautomers of the Schiff base, the former of which should emit at around 390 nm and the latter at around 500 nm (*30*). When excited at 340 nm, intense emission was observed at around 400 nm with minor emission at 500 nm (Fig. 3A), suggesting that the 335-nm absorption band could be the substituted aldamine structure according to the criteria described above (*30*). However, recent studies (*31–33*) showed that emission at a similar wavelength could be obtained from the enolimine structure in the excited state (E* in Scheme 2-1). That is, E* can undergo either proton transfer from the 3′-OH group to imine N in the singlet excited state to yield the excited ketoenamine structure (K*) (route 1 in

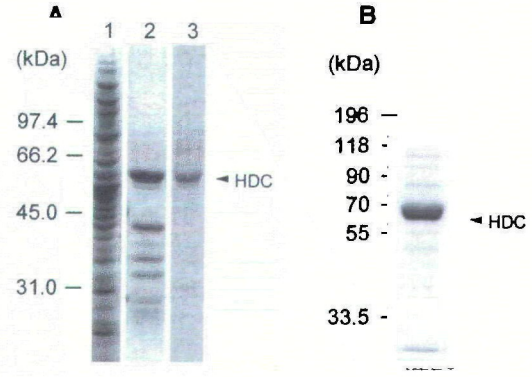

Fig. 1. **Analysis of recombinant 1/512 HDC expression and purification.** Proteins were visualized by Coomassie Brilliant Blue staining. (A) Protein purified from *E. coli* cultures transformed with plasmid pET-11a/HDC1/512. Lane 1, sample collected after Phenyl-Sepharose chromatography; lane 2, sample collected after DEAE-Toyopearl 650M chromatography; lane 3, sample collected after hydroxyapatite chromatography. (B) Protein purified from *E. coli* cultures transformed with plasmid pGEX6P-1/HDC1/512 after excision from the GST domain. The positions of the standard molecular weight marker proteins are shown (numbers indicate the molecular masses of the proteins).

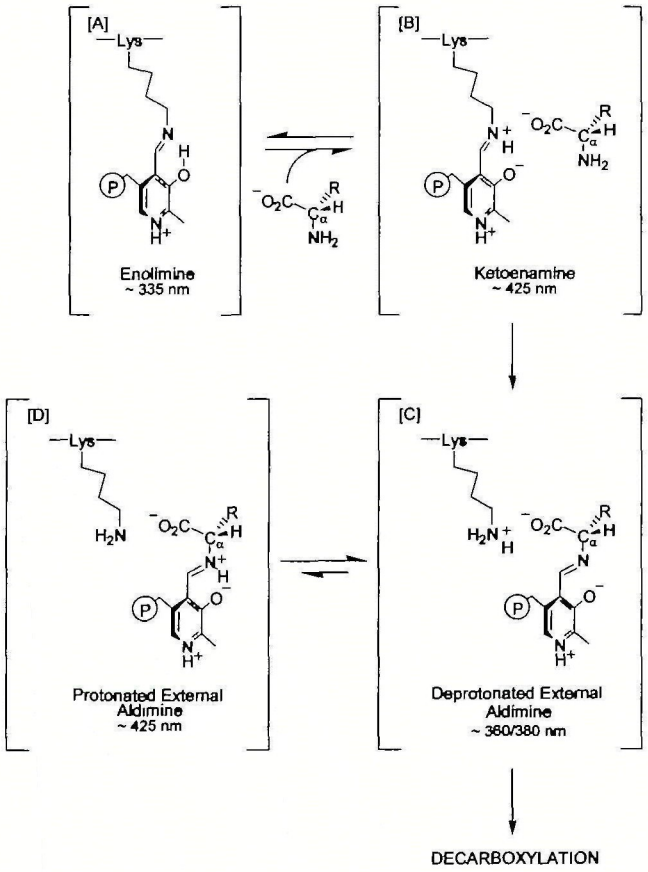

Scheme 1. **Reaction mechanism of HDC with histidine.** The most abundant tautomeric forms of the Schiff bases deduced from the present results are shown. Respective absorption maxima are given below the formulas.

Scheme 2), or radiative decay of the excited state to the ground state E (route 2 in Scheme 2), depending on the acidity of the 3'-OH group *(32)*. K* emits at around 500 nm whereas E*, which has a higher energy level than K*, emits at around 410 nm *(31–33)*. Additionally, the fluorescence excitation spectrum of HDC monitored at the emission wavelength of 390 nm (Fig. 4) shows that the absorption band that gives the excited state is seen at 345–350 nm, which is apparently longer than the wavelength generally observed for substituted aldamine structures, 330–335 nm *(34)*. Therefore, the 400-nm emission from HDC can be considered to result from E*, and not from the substituted aldanine. The shoulder at 500 nm is apparently due to K* formed from E* via intramolecular proton transfer *(8, 33)*. Comparison of the similar intensity of the 500-nm emission in Fig. 3, A and B, and the twofold higher absorption at 335 nm than that at 425 nm (Fig. 2) indicates that the quantum yield of the 500-nm emission on excitation at 340 nm is about half that on excitation at 425 nm. This shows that the partition ratio between routes 1 and 2 from E* is nearly 1:1. This partition ratio is the same as that observed for DDC *(8)*, although there is a significant difference in the intensity of the 500-nm emission between HDC and DDC. This indicates that the acidity of the 3'-OH group is similar between HDC and DDC. The relatively low intensity of the emission at 500 nm from HDC on either 340- or 425-nm excitation as compared to the 400-nm emission on 340-nm excitation is considered to be due to the quenching of the 500-nm emission in the HDC protein, the cause of which, however, is not known at present.

For the aldamine structure, it is important to discuss the possibility of adduct formation of the Schiff base with DTT (SA in Scheme 2-2 is DTT), which is used for purification of the enzyme, since this is the case for HDC from Gram-negative bacteria *(19)* and eukaryotic ODC *(18)*. However, as the binding of thiol compounds to the imine is a reversible reaction *(19)* and the enzyme is gel-filtrated prior to spectroscopic analysis, it is hard to consider that DTT remains bound to the enzyme. A brief chemical consideration indicates that the substituted aldamine structure would be completely inactive. Therefore, even if we assume that a part of the Schiff base forms the aldamine with DTT, the activity of HDC we have detected must have arisen from the enzyme with the Schiff base (not the substituted aldamine) structure. However, the HDC activity was not inhibited by increasing DTT concentration; the activity in the absence of DTT was 1.25 ± 0.03 nkat/mg, compared to the activity observed with 1 mM DTT (1.50 ± 0.08 nkat/mg), 2 mM (1.36 ± 0.14 nkat/mg), or 5 mM (1.47 ± 0.06 nkat/mg). Therefore, we can consider that, unlike the bacterial HDC,

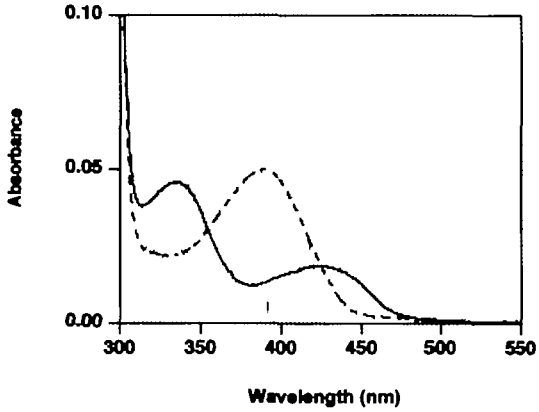

Fig. 2. **Absorption spectra of HDC in the absence (solid line) and presence (dotted line) of 1 mM HisOMe.** The spectra were taken in 50 mM PIPES-NaOH buffer, pH 7, at 25°C. The enzyme concentration was 8 μM.

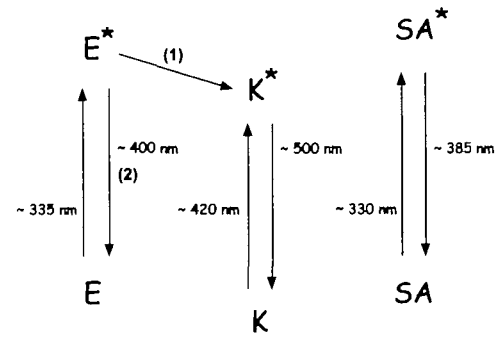

Scheme 2. **Excitation, transition, and radiation of the different tautomeric forms of the PLP Schiff base and aldamine.** E, enolimine form of the Schiff base; K, ketoenamine form of the Schiff base; SA, substituted aldamine; (1) and (2) are two alternative routes for E* decay.

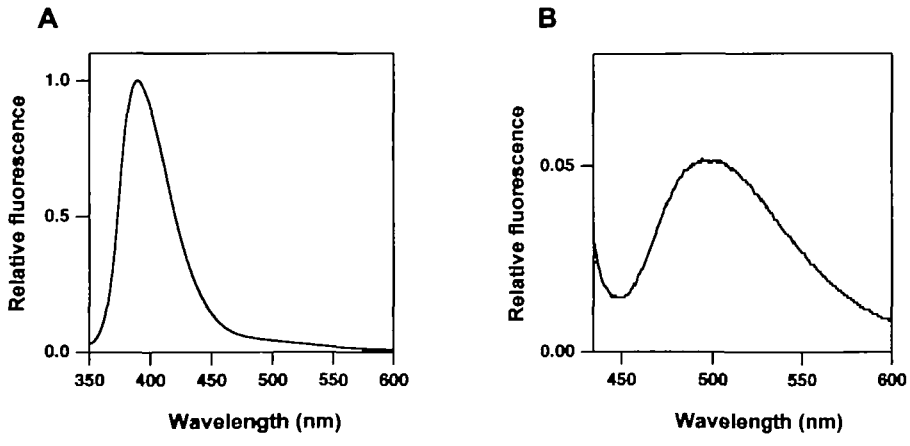

Fig. 3. **Fluorescence spectra of HDC.** The spectra were measured in 50 mM PIPES-NaOH buffer, pH 7, at 25°C. The enzyme concentration was 8 μM. (A) Excitation wavelength of 340 nm. (B) Excitation wavelength of 425 nm.

the mammalian HDC does not form the aldamine structure with DTT.

All of these data indicate that the internal Schiff base of our version of rat HDC is mainly the enolimine tautomer formed between PLP and the ε-amino group of Lys-308 located in an apolar environment, which seems to be more protected from reaction with external nucleophiles than the homologous prokaryotic enzyme. The predominance of the enolimine structure of the internal Schiff base is considered to reflect the hydrophobic nature of its active site that accepts aromatic substrates, just like that of DDC (*8*).

HDC showed only a slight decrease in absorbance at 335 nm, and a simultaneous increase at 425 nm was observed when the pH was changed from 7 to 6. However, the change was too small to be considered to reflect protonation/deprotonation that occurs on the Schiff base moiety. Rather, it should be interpreted as reflecting a slight change in the environment around the Schiff base that could be caused by the change in the charged status of dissociation groups of the enzyme protein (*33*).

Structure of the External Schiff Base—In general catalytic reactions of PLP-dependent enzymes (*35*), after substrate addition, the lysine residue involved in the internal Schiff base (Lys-308 in the case of rat HDC) is displaced by a transaldimination process, which yields a substrate-PLP Schiff base (the external Schiff base). To characterize the external Schiff base generated from the Michaelis complex, we used a substrate analogue, L-histidine methyl ester (HisOMe), containing an esterified carboxyl group that cannot undergo decarboxylation, and the catalytic reaction stops at the step of the external Schiff base. The resultant structure can be a model for the external Schiff base, which is suitable for analysis by conventional spectrophotometry. Figure 2 (dotted line) shows a typical UV/Vis spectrum recorded after adding 1 mM HisOMe to HDC. Binding of HisOMe to HDC decreased the absorbance at both 335 and 425 nm, and dramatically increased the absorbance around 388 nm. Similar results have been observed for rat DDC with DOPA methyl ester as the substrate analogue (*8*). This absorption peak (388 nm) is close to the typical values for the deprotonated Schiff base (360–380 nm), structure C in Scheme 1; and low absorbance was detected at 425 nm (the protonated ketoenamine form named D in Scheme 1).

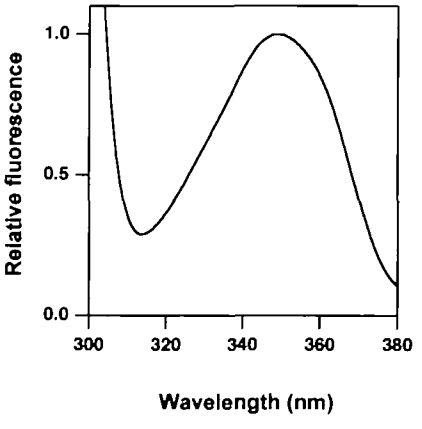

Fig. 4. **Fluorescence excitation spectrum of HDC with emission at 390 nm.** The spectrum was measured in 50 mM PIPES-NaOH buffer, pH 7, at 25°C. The enzyme concentration was 8 μM.

The UV/Vis absorption spectra did not change between pH 6 and 7 (results not shown).

Since observation of the Michaelis complex was not possible using the commercial analogue, we tried to detect it by following the reaction with L-histidine in a stopped-flow spectrophotometer (Fig. 5). Upon mixing the enzyme with histidine, a biphasic spectral change was observed. Thus, in the first fast phase, a rapid increase in the absorbance at 425 nm with a concomitant decrease in the 335-nm peak was observed within 50 ms, showing a shift from the enolimine form to the ketoenamine form of the Schiff base. This tautomeric shift is probably due to electrostatic perturbation in the local environment of the coenzyme on formation of the Michaelis complex, which is most probably caused by the interaction of the internal Schiff base and the substrate α-amino group. These spectral changes are similar to those observed for the reaction of DDC and DOPA (*8*). On the other hand, in a second slower phase, the absorption at both 425 and 335 nm decreased, and there was the concomitant emergence of a new absorption band at around 380 nm within 2.0 s. Unfortunately, the limited amount of HDC obtained prevented us from performing further analysis, such as of the dependency on histidine concentration. However, the emergence of the 380-nm peak in the second slower phase strongly indicates that the 380-nm absorbing species of the external Schiff base (identified in the HisOMe complex) is actually formed in the normal catalytic process. The apparent rate constant for the emergence of the 380-nm species is around 2 s^{-1}. This represents the relaxation process from the Michaelis complex-dominant state to the steady-state that contains both the Michaelis complex and the external Schiff base as dominant species. This value is about 30 times higher[3] than the k_{cat} value (0.077 s^{-1}), which indicates that the catalytic

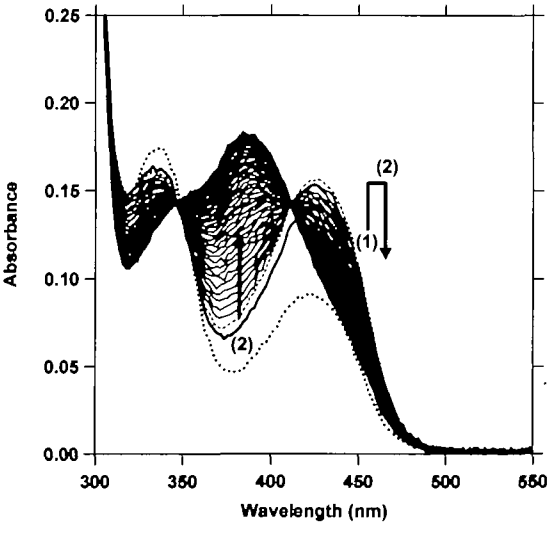

Fig. 5. **Time-resolved spectra for the reaction of HDC and L-histidine.** Enzyme (40 μM) and L-histidine (2 mM) were reacted in 50 mM PIPES–NaOH, pH 7.0, at 25°C. After the addition of L-histidine, spectra were taken between 26.88 ms (bold line spectrum) and 2024 ms at 25.6-ms intervals. The spectrum at 52.48 ms is shown as a dashed line. The bold dotted line represents the spectrum of HDC in the absence of L-histidine. The trends of spectra are indicated by arrows numbered at the beginning: 1, from time 0 to 52.48 ms; 2, from 52.48 ms to 2024 ms.

step(s) after the external Schiff base, including the decarboxylation step, is rate-determining in the entire catalytic reaction.

Conformational Change of the Schiff Base during Transaldimination—More information on the conformational changes of the coenzyme occurring after ligand binding can be obtained by CD spectroscopy. Figure 6 shows CD spectra of HDC (Fig. 6A) and HDC complexed with 1 mM HisOMe (Fig. 6B). The CD spectrum of HDC showed a positive Cotton effect at around both 335 and 425 nm; these wavelengths fit well to the wavelengths of the absorption peaks. Upon the addition of HisOMe, the ellipticity of the enzyme at both 335 and 425 nm disappeared, and a strong negative Cotton effect was observed at 390 nm. In many PLP enzymes, the PLP–lysine Schiff base has a distorted conformation, in which the imine bond is out of the plane of the pyridine ring, that is, the torsion angle (χ) around C4–C4′ is not equal to zero. Torsion angle χ is the major determinant of the Cotton effect observed for the Schiff base absorption band (*36*). Considering the expected similarity of the protein folding patterns, and the alignment of the active-site residues between HDC and aspartate aminotransferase (where $\chi > 0$), we can expect that the positive Cotton effect in the unliganded enzyme reflects a positive χ value of the internal Schiff base in HDC, and the strong negative Cotton effect of the external Schiff base complex with HisOMe reflects a negative χ value. The inversion of the conformation of the Schiff base is probably caused by the change in the amino moiety of the Schiff base from the ε-amino group of Lys308 to the α-amino group of the ligand, these two groups being located on opposite faces of PLP. In the case of DDC with the dopa methyl ester, although a reduction of the positive Cotton effect was observed, no inversion of the Cotton effect was seen (*8*). This indicates that the external Schiff base of HDC has a more distorted structure than that of DDC. This indicates that the conjugation between the imine and the pyridine is lowered in the external Schiff base of HDC as compared with that of DDC. As this conjugation is important for propagation of the electron-withdrawing effect of the pyridine ring to the C(α)–C(carboxylate) bond, the larger torsion angle is expected to lower the catalytic ability of PLP in the decarboxylation step. In this sense, it is interesting to recall the observation that the overall rate constant of the steps after the external Schiff base, which includes the decarboxylation step, is apparently lower for HDC than for DDC (see above). Thus, we can consider that the distorted conformation of the HDC external Schiff base lowers the rate of decarboxylation by partially breaking the π-conjugation between the pyridine ring and the imine.

The recent crystallographic structure of DDC complexed with carbiDOPA can be a model for the external Schiff base of fold type I decarboxylases (*6*). However, the incorporation of an extra N atom between C(α) and aldimine (in this case hydrazone) N requires adjustment of the atoms around the hydrazone. Accordingly, determination of the actual aldimine-pyridine conjugation structure awaits further crystallographic studies on fold type I decarboxylases. For this purpose, the development of a more efficient expression system of HDC, in order to obtain a sufficient amount of the enzyme for further characterization, is anticipated. This is now underway in our laboratory.

Thanks are due to Dr. H. Mizuguchi for the help during the stay of MTO at Osaka Medical College, and to Dr. J.L. Urdiales for that during the preparation of the figures.

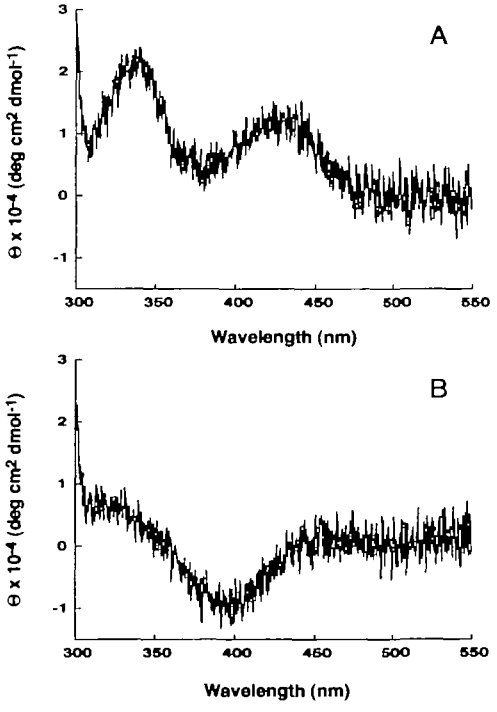

Fig. 6. **Circular dichroism spectra of HDC.** The spectra were taken in 50 mM PIPES-NaOH buffer, pH 7, at 25°C in the absence (A) and presence (B) of 1 mM HisOMe.

REFERENCES

1. Sandmeier, E., Hale, T.I., and Christen, P. (1994) Multiple evolutionary origin of pyridoxal-5′-phosphate-dependent amino acid decarboxylases. *Eur. J. Biochem.* **221**, 997–1002
2. Jansonius, J.N. (1998) Structure, evolution and action of vitamin B6-dependent enzymes. *Curr. Opin. Struct. Biol.* **8**, 759–769
3. Momany, C., Ernst, S., Ghosh, R., Chang, N.L., and Hackert, M.L. (1995) Crystallographic structure of a PLP-dependent ornithine decarboxylase from *Lactobacillus* 30a to 3.0 Å resolution. *J. Mol. Biol.* **252**, 643–655
4. Kern, A.D., Oliveira, M.A., Coffino, P., and Hackert, M.L. (1999) Structure of mammalian ornithine decarboxylase at 1.6 Å resolution: stereochemical implications of PLP-dependent amino acid decarboxylases. *Structure* **7**, 567–581
5. Kern, A., Oliveira, M.A., Chang, N.L., Ernst, S.R., Carroll, D.W., Momany, C., Minard, K., Coffino, P., and Hackert, M.L. (1996) Crystallization of a mammalian ornithine decarboxylase. *Proteins* **24**, 266–268
6. Burkhard, P., Dominici, P., Borri-Voltattorni, C., Jansonius, J.N., and Malashkevich, V.N. (2001) Structural insight into Parkinson's disease treatment from drug-inhibited DOPA decarboxylase. *Nat. Struct. Biol.* **8**, 963–967
7. Dunathan, H.C. and Voet, J.G. (1974) Stereochemical evidence for the evolution of pyridoxal-phsphate enzymes of various function from a common ancestor. *Proc. Natl. Acad. Sci. USA* **71**, 3888–3891
8. Hayashi, H., Mizuguchi, H., and Kagamiyama H. (1993) Rat liver aromatic L-aromatic acid decarboxylase: spectroscopic and kinetic analysis of the coenzyme and reaction intermediates. *Biochemistry* **32**, 812–818
9. Hayashi, H., Tsukiyama F., Ishii S., Mizuguchi, H., and Kagamiyama H. (1999) Acid-basic chemistry of the reaction of aro-

matic L-amino acid decarboxylase and dopa analyzed by transient and steady-state kinetics: preferential binding of the substrate with its amino group unprotonated. *Biochemistry* **38**, 15615–15622
10. Ishii, S., Mizuguchi, H., Nishino, J., Hayashi, H., and Kagamiyama, H. (1996) Functionally important residues of aromatic L-amino acid decarboxylase probed by sequence alignment and site-directed mutagenesis. *J. Biochem.* **120**, 369–376
11. Ishii, S., Hayashi, H., Okamoto, A., and Kagamiyama, H. (1998) Aromatic L-amino acid decarboxylase: conformational change in the flexible region around Arg334 is required during the transaldimination process. *Protein Sci.* **7**, 1802–1810
12. Moore, P.S., Dominici, P., and Borri-Voltattorni, C. (1996) Cloning and expression of pig kidney dopa decarboxylase: comparison of the naturally occurring and recombinant enzymes. *Biochem. J.* **315**, 249–256
13. Nishino, J., Hayashi, H., Ishii, S., and Kagamiyama, H. (1997) An anomalous side reaction of the Lys303 mutant aromatic L-amino acid decarboxylase unravels the role of the residue in catalysis. *J. Biochem.* **121**, 604–611
14. Chu, W. and Metzler D.E. (1994) Enzymatically active truncated cat brain glutamate decarboxylase: expression, purification, and absorption spectrum. *Arch. Biochem. Biophys.* **313**, 287–295
15. Osterman, A.L., Kinch, L.N., Grishin, N.V., and Phillips, M.A. (1995) Acidic residues important for substrate binding and cofactor reactivity in eukaryotic ornithine decarboxylase identified by alanine scanning mutagenesis. *J. Biol. Chem.* **270**, 11797–11802
16. Osterman, A.L., Brooks, H.B., Jackson, L., Abbott, J.J., and Phillips, M.A. (1999) Lysine-69 plays a key role in catalysis by ornithine decarboxylase through acceleration of the Schiff base formation, decarboxylation, and product release steps. *Biochemistry* **38**, 11814–11826
17. Coleman, C.S., Stanley, B.A., Viswanath, R., and Pegg A.E. (1994) Rapid exchange of subunits of mammalian ornithine decarboxylase. *J. Biol. Chem.* **269**, 3155–3158
18. Brooks, H.B. and Phillips, M.A. (1997) Characterization of the reaction mechanism for *Trypanosoma brucei* ornithine decarboxylase by multiwavelenghth stopped-flow spectroscopy. *Biochemistry* **36**, 15147–15155
19. Tanase, S., Guirard, B.M., and Snell, E.E. (1985) Purification and properties of a pyridoxal 5′-phosphate-dependent histidine decarboxylase from *Morganella morganii* AM-15. *J. Biol. Chem.* **260**, 6738–6746
20. Taguchi, Y., Watanabe, T., Kubota, H., Hayashi, H., and Wada, H. (1984) Purification of histidine decarboxylase from the liver of fetal rats and its immunochemical and immunohistochemical characterization. *J. Biol. Chem.* **259**, 5214–5221
21. Engel, N., Olmo, M.T., Coleman, C.S., Medina M.A., Pegg, A.E., and Sánchez-Jiménez, F. (1996) Experimental evidence for structure/function features in common between mammalian histidine decarboxylase and ornithine decarboxylase. *Biochem. J.* **320**, 365–368
22. Viguera, E., Trelles, O., Urdiales, J.L., Matés, J.M., and Sánchez-Jiménez, F. (1994) Mammalian L-amino acid decarboxylases producing 1,4-diamines: analogies among differences. *Trends Biochem. Sci.* **19**, 318–319
23. Olmo, M.T., Urdiales, J.L., Pegg, A.E., Medina, M.A., and Sánchez-Jiménez, F. (2000) *In vitro* study of proteolytic degradation of rat histidine decarboxylase. *Eur. J. Biochem.* **267**, 1527–1531
24. Ohmori, E., Fukui, T., Imanishi, N., Yatsunami, K., and Ichikawa, A. (1990) Purification and characterization of L-histidine decarboxylase from mouse mastocytoma P-815 cells. *J. Biochem.* **107**, 834–839
25. Dartsch, C., Chen, D., Hakanson, R., and Persson, L. (1999) Multiple forms of rat stomach histidine decarboxylase may reflect post-translational activation of the enzyme. *Regul. Peptides* **81**, 41–48
26. Fleming, J.W. and Wang, T.C. (2000) Amino and carboxyterminal PEST domain mediate gastrin stabilization of rat L-histidine decarboxylase isoforms. *Mol. Cell Biol.* **20**, 4932–4947
27. Fajardo, I., Urdiales, J.L., Medina, M.A., and Sánchez-Jiménez, F. (2001) Effects of phorbol ester and dexamethasone treatment on histidine decarboxylase and ornithine decarboxylase in basophilic cells. *Biochem. Pharmacol.* **61**, 1101–1106
28. Kuramitsu, S., Hiromi, K., Hayashi, H., Morino, Y., and Kagamiyama, H. (1990) Pre-steady state kinetics of *Escherichia coli* aspartate aminotransferase catalyzed reactions and thermodinamic aspects of its substrate specificity. *Biochemistry* **29**, 5469–5476
29. Yamamoto, J., Fukui, T., Suzuki, K., Tanaka, S., Yatsunami, K., and Ichikawa, A. (1993) Expression and characterization of recombinant mouse mastocytoma histidine decarboxylase. *Biochim. Biophys. Acta* **1216**, 431-440
30. Johnson, G.F., Tu, J.I., Bartlett, M.L., and Graves, D.J. (1970) Physical-chemical studies on the pyridoxal phosphate binding site in sodium borohydride-reduced and native phosphorylase. *J. Biol. Chem.* **245**, 5560–5568
31. Honikel, K.O. and Madsen, N.B. (1972) Comparison of the absorbance spectra and fluorescence behavior of phosphorylase b with that of model pyridoxal phosphate derivatives in various solvents. *J. Biol. Chem.* **247**, 1057–1064
32. Vazquez Segura, M.A., Donoso, J., Munoz, F., Blanco, F.G., Garcia del Vado, M.A., and Echevarria, G. (1994) Photophysical study of the Schiff bases of 5′-deoxypyridoxal and *n*-hexylamine in cationic micelles. *Photochem. Photobiol.* **60**, 399–404
33. Zhou, X., and Toney, M.D. (1999) pH studies on the mechanism of the pyridoxal phosphate-dependent dialkylglycine decarboxylase. *Biochemistry* **38**, 311–320
34. Kallen, R.G., Korpela, T., Martell, A.E., Matsushima, Y., Metzler, C.M., Metzler, D.E., Morozov, Y.V., Ralston, I.M., Savin, F.A., Torchinsky, Y.M., and Ueno, H. (1985) in *Transaminases* (Metzler, D.E. and Christen, P., eds) pp. 37–108, John Wiley & Sons, New York
35. Hayashi, H. (1995) Pyridoxal enzymes: mechanistic diversity and uniformity. *J. Biochem.* **118**, 463–473
36. Hayashi, H., Mizugushi, H., and Kagamiyama, H. (1998) The imine-pyridine torsion of the pyridoxal 5'-phosphate Schiff base of aspartate aminotransferase lowers its pK_a in the unliganded enzyme and is crucial for the successive increase in the pK_a during catalysis. *Biochemistry* **37**, 15076–15085